Fabrication of Supported Mesoporous TiO_2 Membranes: Matching the Assembled and Interparticle Pores for an Improved Ultrafiltration Performance

Wenheng Jing,* Wei Huang, Weihong Xing,* Yong Wang, Wanqin Jin, and Yiqun Fan

State Key Laboratory of Materials-Oriented Chemical Engineering, College of Chemistry and Chemical Engineering, Nanjing University of Technology, Nanjing 210009, Jiangsu, China

ABSTRACT We report the fabrication and ultrafiltration performances of an asymmetric composite membrane with a mesoporous TiO_2 skin layer coated on a macroporous alumina support. Mesoporous TiO_2 was first prepared and deposited on the substrate through a sol−gel process where a ethylene oxide and propylene oxide triblock polymer (PEO−PPO−PEO, P123) was used to modify the properties of the sols and also to introduce assembled pores in the skin layer. The obtained mesoporous TiO_2 membrane was characterized by means of scanning electron microscopy, transmission electron microscopy, X-ray diffraction, and nitrogen adsorption. We found that there were two types of wormlike mesopores present in the TiO_2 membrane: interparticle and assembled pores. By carefully controlling the sol properties, we made the two types of pores match each other, which means the size of the interparticle pores is close or smaller than that of the assembled pores. This pore-size matching ensures a narrow pore-size distribution and, consequently, a good retention performance of the obtained TiO_2 membrane. The pore size of the TiO_2 membrane is ca. 6 nm, as revealed by both nitrogen adsorption and dextran separation experiments, and it has a pure water flux of 7.12 $L/(m^2 \cdot h \cdot bar)$ and a cutoff molecular weight of 19 000 Da, which is very attractive for applications in the enrichment and separation of proteins and polypeptides.

KEYWORDS: asymmetric membrane • mesoporous titania • ultrafiltration • self-assembly

INTRODUCTION

Membrane-based separation and purification processes have been becoming increasingly attractive in industries because of their cost-effective and energy-efficient advantages over other methods. Mesoporous membranes with pore sizes ranging from 2 to 50 nm are particularly significant because they find extensive applications for ultrafiltration of proteins, colloids, and macromolecules with molecular weights from ca. 10K up to 1000K (1, 2), and inorganic mesoporous membranes are practically appealing because of their superior chemical resistance to acid, organic solvents, etc., which makes them still workable in some harsh operating environments (3). Mesoporous molecular sieves, e.g., MCM-48, having narrow pore-size distributions and tunable pore sizes ranging from 2 to 10 nm, are "ideal" ultrafiltration materials provided that they can be fabricated to form continuous membranes with pores running through the entire membrane thickness. Although most efforts are dedicated to silica-based mesoporous molecular sieves, from a practical point of view they are not perfectly suitable for ultrafiltration applications because their relatively low hydrothermal and chemical stability will not only limit their applications in many situations but, more importantly, hinder the chemical cleaning process for membrane defouling, which is essential for the stable running of the membrane separation process (4).

Al_2O_3, TiO_2, and ZrO_2 are the most common, chemically stable, ceramic membrane materials (5, 6), among which TiO_2 mesoporous membranes have gained tremendous popularity because of their photocatalytic activity (7, 8) in addition to their superior chemical resistance. Typically, the colloid sol−gel route is used in the fabrication of TiO_2 mesoporous membranes (9, 10). The mesostructures of the TiO_2 membranes are not easy to control because they require the most reactive alkoxide, which is hard to handle (11), and it is difficult to stabilize the small particles (12); as a result, membranes obtained generally have a wide pore-size distribution (3).

In the sol−gel process for the preparation of a TiO_2 mesoporous membrane, usually polymeric additives will be added to stabilize the sols, and two types of polymeric additives can be used. One is water-soluble polymers, e.g., cellulose and poly(vinyl alcohol) (PVA). They merely deliver their function to cover the sols and thicken the sol−gel system. However, the addition of this type of polymer often leads to the formation of relatively large particles, and as a result, membranes with wider pore-size distribution and worse rejection performance are usually produced (13). The other one is more active amphiphilic polymers, e.g., ethylene oxide and propylene oxide triblock polymers (PEO−PPO−PEO). These polymers will be dissolved in water as

* Corresponding author. Tel: +86-25-8317 2288. Fax: +86-25-8317 2292. E-mail: jingwenheng@yahoo.com.cn (W.J.), xingwh@njut.edu.cn (W.X.).
Received for review May 11, 2009 and accepted June 18, 2009

DOI: 10.1021/am900246m

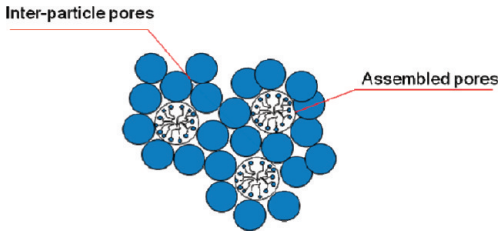

FIGURE 1. Schematic diagram of the forming interparticle and assembled pores.

micelles because of their amphiphilic nature, with hydrophilic PEO chains extended in water as the corona and hydrophobic PPO chains collapsed in the core, which will stabilize the sol, on the one hand. On the other hand, more importantly, the ethylene oxide chains will interact with metal species on the surface of the sol, directing the arrangement of the final TiO_2 particles in a more or less ordered way, other than the random packing in the case of using plain polymeric additives. This is actually the well-known, so-called "self assembly" process of TiO_2 sols directed by the triblock polymer. After the polymer is burned off, there are two sets of pore structures: one is the interparticle pores formed between randomly packed neighboring particles, and the other one is the assembled pores, which are the position preoccupied by triblock polymer micelles. Therefore, there will be more pores or, in other words, the porosity of the final membranes increases compared with the system using plain polymers. Figure 1 shows the schematic diagram of forming interparticle and assembled pores. Because there are two sets of pores, it is necessary to adjust the sol−gel conditions to make the two sets of pores match each other in order to keep the narrow size distribution. To this end, we should be very careful in determining the molecular weights and volume fractions of the constituent blocks of the triblock copolymer to be used in the sol−gel process because they significantly influence not only the dimension of the sol but also the micelle size, which, in turn, dictates the diameter of the assembled pores. Moreover, the percentages of triblocks and other sol−gel process parameters are also playing a role in the formation of both pores, which should also be taken into account when optimizing the sol−gel process for the preparation of membranes with narrow pore-size distribution. The size of the assembled pores from PEO−PPO−PEO triblock polymers usually falls in the range of several nanometers to 10 nm (14, 15) and is featured as monodisperse. However, for the interparticle pores, their size is dependent on the constitutive particles and typically has a relatively wide distribution. If the average size of the interparticle pores is smaller than, or in an "ideal" case, identical with that of assembled pores, which means the two sources of pores "match" each other, the retention performance of the membrane will be determined mainly by the assembled pores and is expected to be much better than the reverse case, where the interparticle pores are larger.

There are many efforts aiming to fabricate mesoprous titania materials in the form of films, fibers, or powders using a PEO−PPO−PEO triblock polymer to direct the sol−gel process in which the evaporation-induced self-assembly (EISA) is frequently involved (16−20). For instance, Choi et al. prepared mesoporous TiO_2 thin films with well-defined 2D hexagonal mesopores on thick, nonporous glass substrates (21). However, in order to obtain a robust separation membrane with enhanced flux and a good rejection performance, the mesoporous TiO_2 layer should be formed on a macroporous support to have an asymmetric composite membrane configuration where the mesoporous TiO_2 layer serves as the separation skin layer and the macroporous support as the substrate to provide mechanical stability and to reduce the filtration resistance. Unfortunately, direct coating of the sols onto macroporous supports failed because the fluidal sols tend to penetrate into and fill the support macropores. To solve this problem, large amounts of polymeric additives sometimes are introduced into the sols to increase their viscosity and prevent their penetration into the support pores, but this, on the other hand, violently influences the particle size of the sols and, as a result, deteriorates the pore-size distribution in the skin layer of the composite membrane.

In this work, we propose an improved EISA approach for the preparation of asymmetric mesoporous TiO_2 membranes. Our strategy is to use a $(EO)_{20}(PO)_{70}(EO)_{20}$ (P123) structure-directing agent to form assembled pores and to make EISA occur at a relatively high temperature and a relatively low humidity (RH), which is demonstrated to be helpful for the prevention of sols to be penetrated into the supports and the quick formation of a thin gel layer on the surface of the supports. TiO_2 polymeric sols with smaller particle size can be formed by controlling the amount of P123 added into the sol, which makes the interparticle pores have sizes similar to those of the assembled pores. This size match of the two sets of pores ensures a narrow pore-size distribution of the final membrane. Pure water and dextran solution filtration tests were also carried out to examine the ultrafiltration performance of the obtained asymmetric membrane.

EXPERIMENTAL SECTION

Materials. Tetrabutyl titanate, acetylacetone, and 1-butanol with a purity of 99% obtained from Shanghai Lingfeng Chemical Reagent Co. Ltd. and nitric acid with a concentration of 68% purchased fromYangzhou Hubao Chemical Reagents Corp. were used without further purification. The triblock copolymer $(EO)_{20}(PO)_{70}(EO)_{20}$ (P123) with a molecular weight of 5800 was purchased from Sigma-Aldrich and used as received.

Synthesis of Sol. A total of 6.5 g of P123 was dissolved in 18 mL of 1-butanol to get a clear solution, and to the polymer solution were added 17 mL of tetrabutyl titanate and 2.5 mL of acetylacetone. The obtained mixture was then combined with another solution composed of 9 mL of 1-butanol, 0.7 mL of nitric acid, and 2.7 mL of deionized water. The final mixture was subsequently stirred at 32 °C for 4 h, and the mass concentration of P123 in the solution was 12.1 wt %. Sols without P123 were also prepared using the same recipe as that described above while the part with P123 was replaced by the same amount of 1-butanol.

Preparation of Unsupported Membranes. The fresh sol was first poured into a Petri dish to form a liquid layer with an approximate thickness of 1−2 mm, which was then aged at 60

°C and a RH of 35% for 12 h. The obtained gel was then calcined at 400 °C for 200 min in air to burn off the polymer template. Sols without P123 were also subjected to the same procedure to obtain corresponding unsupported membranes.

Preparation of Supported Membranes. An alumina support with a macroporous structure was first prepared. An alumina powder with an average size of 2.6 μm was mixed with poly(vinyl alcohol) (PVA) and paraffin and then pressed at 8 MPa for 60 s. The pressed disks were finally sintered at 1350 °C to get robust supports. The diameter, thickness, and pore size of the alumina supports were 28.5 mm, 2.2 mm, and 0.13 μm, respectively. The alumina supports were then pretreated using PVA to prevent permeation of the sol into the supports according to the reported method (3). The P123-containing sol was spin-coated on alumina supports at 3000 rpm for 20 s. After the spin coating, the aging and calcining procedures were performed, following the same procedure for treatment as that of the unsupported membranes. This spin-coating, aging, and calcining cycle was repeated three times to obtain crack-free TiO_2 membranes supported on alumina.

Characterization. The particle size distribution of the sols was measured using a Zetasizer 3000. The Brunauer–Emmett–Teller (BET) surface area (S_{BET}), pore volume, and pore-size distribution were determined using a BELSORPII nitrogen adsorption–desorption apparatus. Wide-angle X-ray diffraction (WAXRD) patterns were obtained on a Bruker D8 Advance X-ray diffractometer with Cu Kα radiation ($\lambda = 0.154$ nm) at 40 kV and 30 mA. The transmission electron microscopy (TEM) examinations were performed on a JEM-2100 high-resolution transmission electron microscope. An environmental scanning electron microscope (Quanta 200) was used to measure the thickness of the membrane and to observe the surface morphology of the TiO_2 membrane. The pure water flux and dextran retention of the prepared TiO_2/Al_2O_3 composite membrane were performed according to the ASTM E 1343-90 method. The pure water was pressurized at a transmembrane pressure ranging from 0.3 to 0.8 MP, and 1 g/L dextran (Fluka) solutions with different molecular weights (6000, 70 000, 100 000, and 500 000 Da) were pressurized at a transmembrane pressure of 0.5 MP to determine the cutoff molecular weight of the membrane. The concentrations and molecular weights of dextrans in the raw solutions and permeates were analyzed via a gel permeation chromatography method (Waters Corp.).

RESULTS AND DISCUSSION

A stable sol with small and uniform size is essential for the preparation of a composite membrane with a good separation performance, and P123 is a key component in the sol in our work. Because P123 is dual functional (thickening and structure-directing), the amount of P123 added to the sol greatly influences the properties of the sol and the performance of the final membranes. Sol without polymeric additives has a viscosity of about 3 mPa·s, which is too low to restrain the penetration into the macroporous support in the fabrication of the asymmetric membrane. We found that when 12.1 wt % P123 was introduced into the sol, the viscosity of the sol increased to about 10 mPa·s, suitable for coating on the support. On the other hand, the addition of a polymer additive into the sol will usually increase the particle size of the sol and frequently also widen the particle size distribution, which is highly undesired in the preparation of a separation membrane. Therefore, we use a size analyzer to check the particle size and particle size distribution of the sol with 12.1 wt % P123 and without P123. As shown in Figure 2, the sol without P123 has a narrow particle size

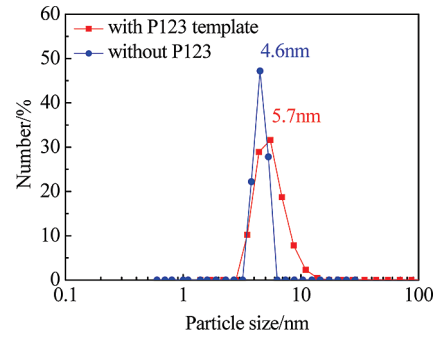

FIGURE 2. Particle size distribution of sols formed without a P123 template (a) and with a 12.1 wt % P123 template (b).

distribution and an average particle size of 4.6 nm, and for the sol with 12.1 wt % P123, although the particle size increases to 5.7 nm, the particle size distribution is just slightly enlarged while for the sols with PVA or other plain polymers as additives, the particle size distribution is deteriorated significantly. When P123 was introduced into the sol system, the tetravalent titanium associated preferentially with the hydrophilic PEO to form crown-ether-type complexes. These complexes have a specific mesostructure through hydrogen bonding and van der Waals forces (22), which increases both the sol viscosity and the particle size in the sol.

Typically, the EISA process is carried out at relatively low temperature, e.g., 20 °C, and high RH, e.g., 80%, to obtain structurally well-ordered mesoporous TiO_2 materials (21), but it is unsuitable for the preparation of asymmetric membranes in the current work. This typical EISA method will lead to hydrolysis in the polymeric gel faster than condensation, resulting in the formation of $TiO_2 \cdot xH_2O$ particles (12) and a very long aging time. In this study, we first spin-coated the P123-containing sols onto the macroporous alumina and then evaporated the sols at a temperature of 60 °C and a RH of 35%, during which gelation of the sol quickly happened on the surface of the support. After coating, gelation, and calcination three times, crack-free membranes were successfully obtained. The resulting membrane possesses an asymmetric structure composed of a skin TiO_2 layer with mesopores. The scanning electron microscopy (SEM) image in Figure 3a shows that the surface of the membrane is homogeneous throughout the whole area and no defects and cracks can be found. Figure 3b shows the cross-sectional SEM image of the composite membrane. The thin TiO_2 layer with an approximate thickness of 3 μm can be seen clearly on the right side of the composite membrane.

Figure 4a shows that the sample possessed wormlike, interconnected channels instead of hexagonally arranged mesopores, which is a consequence of the quick gelation, in which the self-assembly of P123 micelles is not fully developed (23). However, from the point of view of membrane separation, the wormlike pores that are connected with each other will facilitate the diffusion and flow of liquid inside the pores and therefore are more desired than individually separated pores although they may be arranged in an ordered way. The high-resolution TEM image (Figure

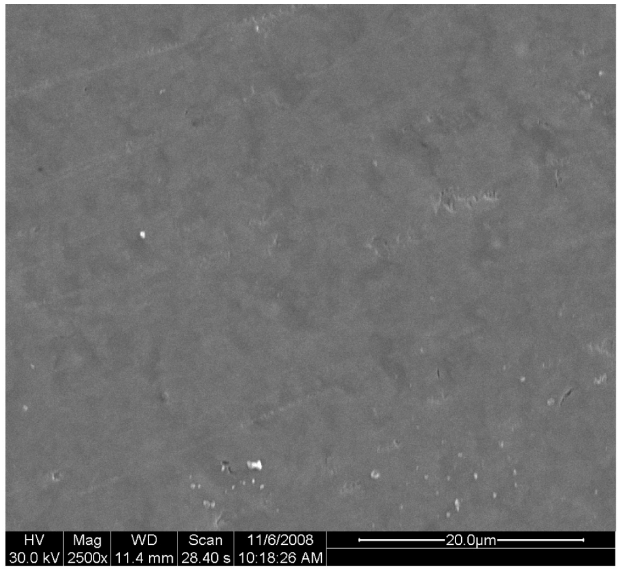

(a)

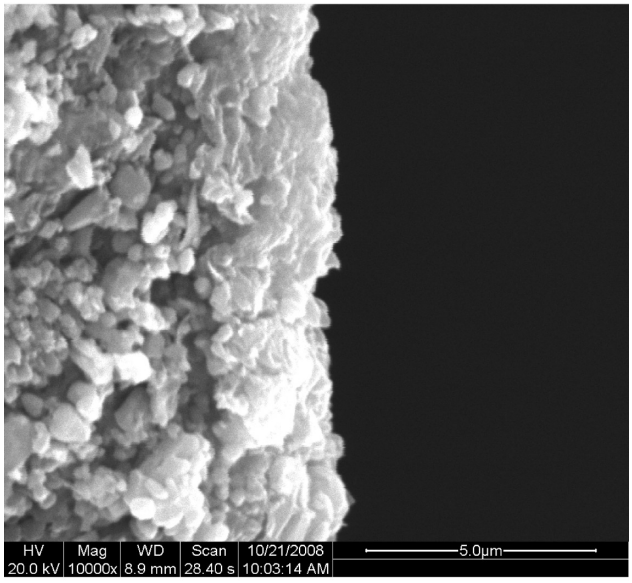

(b)

FIGURE 3. SEM images of the surface (a) and cross section (b) of the composite TiO_2/Al_2O_3 membrane.

4b) shows the existence of many nanocrystals with anatase lattice fringes, and the particle size is about 7 nm, which is small and suitable for the preparation of a mesoporous membrane with small interparticle pores. WAXRD was carried out on unsupported samples from sols without P123 and with 12.1 wt % P123. As shown in Figure 5, either with or without the presence of P123 in the sols, the obtained membranes are crystalline and in the anatase type, while the peaks become wider for the membrane derived from sols with P123. Using the Sherrer formula, the particle sizes of the titania nanocrystals are calculated to be 9.9 and 6.3 nm, respectively, for membranes from sols without P123 and with 12.1 wt % P123, which indicates that the P123 template has restrained the growth of the TiO_2 crystals.

Figure 6a shows nitrogen adsorption−desorption isotherms of the unsupported membrane samples from sols with and without P123. The sample from the P123-containing sol exhibits a type-IV isotherm, which is representative of a mesoporous structure. Figure 6b demonstrates the

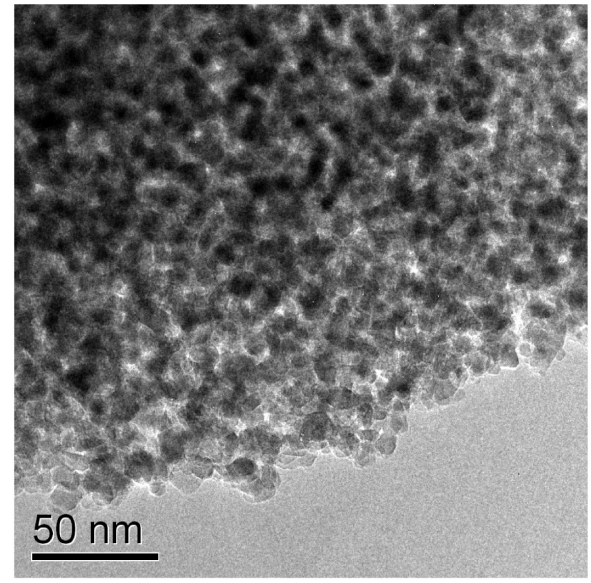

(a)

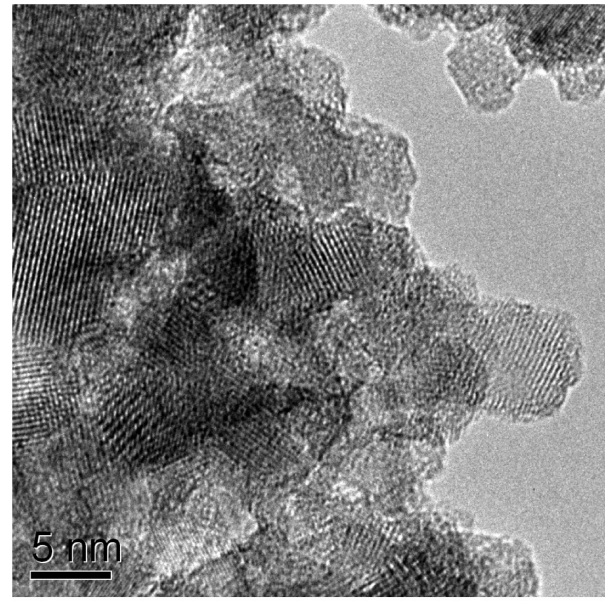

(b)

FIGURE 4. TEM images of the unsupported membrane derived from sols with 12.1 wt % P123.

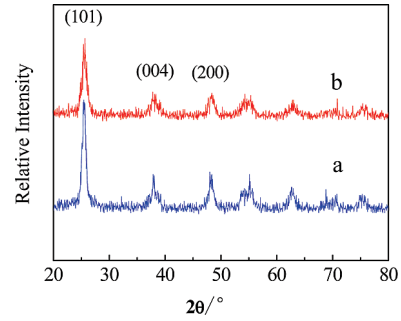

FIGURE 5. WAXRD patterns of unsupported membranes from sols without P123 (a) and with 12.1 wt % P123 (b).

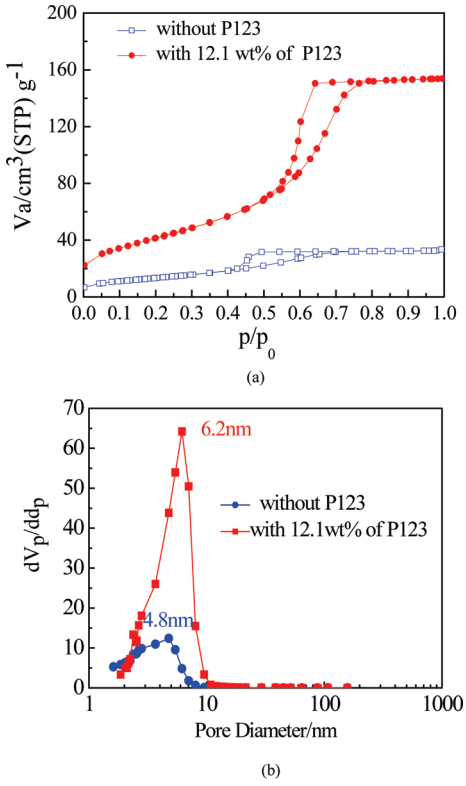

FIGURE 6. Nitrogen adsorption−desorption isotherms (a) and BJH pore-size distribution curves (b) calculated from the adsorption branch of the membrane from sols without P123 and with P123.

Barrett−Joyner−Halenda (BJH) pore-size distribution curves of the samples calculated from the adsorption branch, which implies that the pore size can be inflected by the addition of the P123 template. Because of the small size of the TiO_2 particles, both samples display a very narrow pore-size distribution, which shifts from 1−8 to 2−10 nm after introduction of P123 in the sol. However, the membrane sample obtained from P123-containing sols has a larger average pore size (6.2 nm), increased pore volume (0.25 $cm^3\ g^{-1}$), and a bigger specific surface area (153.6 $m^2\ g^{-1}$), while for the sample from sols without P123, the three values are 4.8 nm, 0.05 $cm^3\ g^{-1}$, and 48.5 $m^2\ g^{-1}$, respectively. The main reason for the improvement of the porosity in the membrane from P123-containing sols is the presence of another type of pore, which is defined by P123 micelles in the sol. In addition, because the TiO_2 nanocrystals are very small and uniform in size, the interparitcle pores are, consequently, small; therefore, the retention performance of the final membrane is largely defined by the assembled pores, and the interparticle pores mainly contribute to the enhancement of the liquid flux.

Finally, we examined the filtration performances of the mesoporous TiO_2 membrane supported on a macroporous alumina. Figure 7 shows the pure water flux and dextran rejection of the alumina support and TiO_2/Al_2O_3 composite membrane. As expected, there is an evident drop in the pure water flux for the composite membarane, which decreased from 16.65 $L/(m^2 \cdot h \cdot bar)$ for the alumina support to 7.12 $L/(m^2 \cdot h \cdot bar)$ for the membrane, but this is still good enough considering the fact that a dense layer of TiO_2 particles was

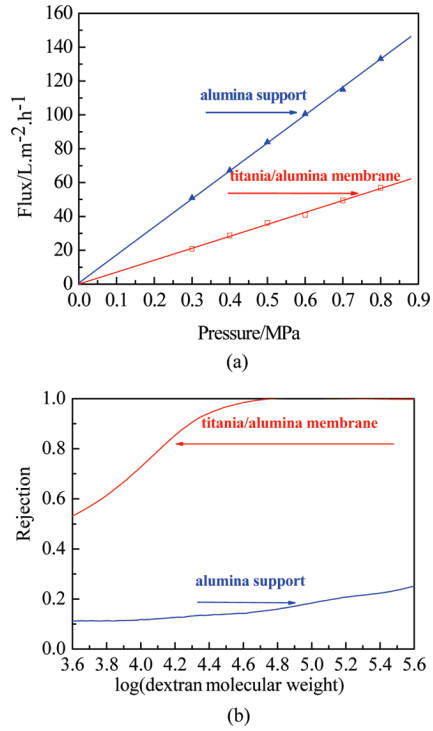

FIGURE 7. Pure water flux (a) and dextran rejection (b) of the alumina support and TiO_2/Al_2O_3 composite membrane.

coated on the surface of the support. In addition, in order to evaluate the performance of membrane separation, filtrations for separating the dextran solution were also investigated. The rejection ratios of the support and membrane are shown in Figure 7b. It is clear that the alumina support has a very poor retention to dextrans with low and medium molecular weights. In contrast, the composite membrane has a good reject effect on the dextran solution, and its cutoff molecular weight is 19 000 Da, which is equivalent to a molecular diameter of approximately 6.1 nm calculated from the formula $r = 0.033\ M^{0.46}$ (8, 24). This value is in good consistency with the pore size estimated using the adsorption branch of the isotherm and BJH models.

CONCLUSIONS

In this study, we demonstrated a simple and effective synthetic method for the fabrication of crack-free, asymmetric mesoporous TiO_2 membranes, which possess narrow pore-size distribution and high pore volume, by matching the assembled and interparticle pores. Amphiphilic PEO−PPO−PEO (P123) polymer was introduced in the TiO_2 sol for the purposes of stabilization and structure-directing. The concentration of P123 is 12.1 wt %, at which the sol is thick enough to suppress sol penetration into the macroporous alumina support, and the particle size distribution of the sol is not obviously deteriorated, which is beneficial to obtain membranes with narrow pore-size distribution. A crack-free layer of TiO_2 on the macroporous support can be obtained after three cycles of spin coating, quick aging, and calcination. TEM examinations revealed the presence of wormlike pores in the TiO_2 membrane, and the membrane is composed of small and uniform anatase TiO_2, which makes the

interparticle pores match the assembled pores. The resulting membrane has a narrow pore-size distribution, large pore volume, and good ultrafiltration properties with a pure water flux of 7.12 L/($m^2 \cdot h \cdot bar$) and a cutoff molecular weight of 19 000 Da.

Acknowledgment. This work is supported the key program of the National Natural Science Foundation of China (20636020), National Basic Research Program of China (2009CB623403), and National High Technology Research and Development Program of China (No. 2006AA03Z534).

REFERENCES AND NOTES

(1) Bowen, W. R.; Williams, P. M. *Adv. Colloid Interface Sci.* **2007**, *134/135*, 3.
(2) Charcosset, C. *Biotechnol. Adv.* **2006**, *24*, 482.
(3) Kim, Y. S.; Yang, S. M. *Adv. Mater.* **2002**, *14*, 1078.
(4) Wu, S. F.; Yang, J. H.; Lu, J. M.; Zhou, Z. H.; Kong, C. L.; Wang, J. Q. *J. Membr. Sci.* **2008**, *319*, 231.
(5) Chang, C. H.; Gopalan, R.; Lin, Y. S. *J. Membr. Sci.* **1994**, *91*, 27.
(6) Larbot, A.; Fabre, J. P.; Guizard, C.; Cot, L. *J. Am. Ceram. Soc.* **1989**, *72*, 257.
(7) Hyun, S. J.; Kang, B. S. *J. Am. Ceram. Soc.* **1996**, *79*, 279.
(8) Ding, X. B.; Fan, Y. Q.; Xu, N. P. *J. Membr. Sci.* **2006**, *270*, 179.
(9) Wu, L. Q.; Huang, P.; Xu, N. P.; Shi, J. *J. Membr. Sci.* **2000**, *173*, 263.
(10) Ju, X. S.; Huang, P.; Xu, N. P.; Shi, J. *J. Membr. Sci.* **2000**, *166*, 41.
(11) Imhof, A.; Pine, D. J. *Nature* **1997**, *389*, 948.
(12) Puhlfürss, P.; Voigt, A.; Weber, R.; Morbé, M. *J. Membr. Sci.* **2000**, *174*, 123.
(13) Alem, A.; Sarpoolaky, H.; Keshmiri, M. *J. Eur. Ceram. Soc.* **2009**, *29*, 629.
(14) Wan, Y.; Yang, H. F.; Zhao, D. Y. *Acc. Chem. Res.* **2006**, *39* (7), 423.
(15) Cho, E. B.; Kim, D.; Jaroniec, M. *J. Phys. Chem. C* **2008**, *112*, 4897.
(16) Brinker, C. J.; Lu, Y. F.; Sellinger, A.; Fan, H. Y. *Adv. Mater.* **1999**, *11*, 579.
(17) Soler-Illia, G. J. de A. A.; Louis, A.; Sanchez, C. *Chem. Mater.* **2002**, *14*, 750.
(18) Andersson, N.; Kronberg, B.; Corkery, R.; Alberius, P. *Langmuir* **2007**, *23*, 1459.
(19) Dong, W. Y.; Sun, Y. Y.; Lee, C. W.; Hua, W. M.; Lu, X. C.; Shi, Y. F.; Zhang, S. C.; Chen, J. M.; Zhao, D. Y. *J. Am. Chem. Soc.* **2007**, *129*, 13894.
(20) Kim, Y. J.; Lee, Y. H.; Lee, M. H.; Kim, H. J.; Pan, J. H.; Lim, G. I.; Choi, Y. S.; Kim, K. K.; Park, N. G.; Lee, C. M.; Lee, W. I. *Langmuir* **2008**, *24*, 13225.
(21) Choi, S. Y.; Mamak, M.; Coombs, N.; Chopra, N.; Ozin, G. A. *Adv. Funct. Mater.* **2004**, *14*, 335.
(22) Yang, P. D.; Zhao, D. Y.; Margolese, D. I.; Chmelka, B. F.; Stucky, G. D. *Nature* **1998**, *396*, 152.
(23) Crepaldi, E. L.; Soler-Illia, G. J. de A. A.; Grosso, D.; Cagnol, F.; Ribot, F. O.; Sanchez, C. *J. Am. Chem. Soc.* **2003**, *125*, 9770.
(24) Granath, K.; Kwist, B. *J. Chromatogr.* **1967**, *28*, 69.

AM900246M